www.czasopisma.pan.pl PAN POLSKA AKADEMIA NAUK www.journals.pan.pl

Arch. Metall. Mater. **64** (2019), 4, 1563-1568

DOI: 10.24425/amm.2019.130127

A. URBAŃCZYK-GUCWA*#, A. BRZEZIŃSKA*, B. ADAMCZYK-CIEŚLAK**, K. RODAK*

CRYSTALLOGRAPHIC TEXTURE AND GRAIN REFINEMENT IN THE CuCr ALLOY DEFORMED BY SPD METHOD

Microstructure and texture of the CuCr0.6 alloy processed by rolling with cyclic movement of rolls (RCMR) at room temperature were investigated. The RCMR processing was applied for the samples in different initial conditions in the solid solution followed by quenching into iced water at 1000°C for 3 h and in aging treatment conditions performed at 500°C for 2 h and at 700°C for 24 h. Application of the solution and aging processes prior to RCMR deformation results in the partial dissolution of Cr particles into the Cu matrix and precipitation of the second phase particles. RCMR processing with value of the total effective strain (ε_{ft}) of 5 was introduced to the material. It was found that the RCMR method is effective in texture weakening. The obtained results revealed that there is a large similarity in texture orientations after RCMR processing independently of heat treatment conditions. Cyclic character of deformation leads to an incomplete transition of LAB to HAB.

Keywords: Severe plastic deformation, Heat treatment, Microstructure, Texture, CuCr0.6 alloy

1. Introduction

During the past several decades, extensive researches have been carried out in the field of materials science and manufacturing engineering to produce materials of high performance capabilities [1-3]. It has been reported that there are many advantages of copper and copper alloys for electric and electronic applications [2,4]. The Cu alloys, especially CuCr0.6 (C18200) are used in numerous applications where excellent combination of mechanical strength and electrical conductivity is required [1,5,6]. In recent years research on the severe plastic deformation (SPD) processing, structure and mechanical behavior of ultrafine grained (100 nm < d < 1 μm) materials are performed [2,7,8]. The obtained results showed great possibilities for fabricating high-strength and ductile Cu alloys [2,9]. The obtained microstructure is complex and depend on initial structure (heat treatment conditions) and deformation parameters as: effective strain or deformation mode. Deformation mode has a strong effect on textural hardening [8,10]. Many works dedicated various SPD techniques and conditions present different phenomenological models for development of high angle boundaries and structure refinement [3,10]. Microstructural observations have provided evidence that grain refinement is realized by continuous evolution in dislocation structure by crystallographic glide at low and moderate strains [1,11]. Another approach describes SPD processes as discontinuous evolution due to localized flow inside shear bands of non-crystallographic orientations [11,12]. A multi-slip activity inside shear bands can promote texture randomization [11,13]. Usually, is considered that HABs are formed discontinuously by grain decomposition into deformation bands [11]. Generally, formation of UFG structures manifests itself in microstructural and textural hardening [2,10]. It is known, that for SPD processed materials microstructural hardening may be insignificant in comparison with textural hardening [14-17].

The RCMR belongs to cyclic methods of SPD and has been previously demonstrated as an effective technique for grain refinement [18-20]. The CuCr0.6 alloy is kind of precipitation-hardened alloys, therefore the problem of initial structure (after applying solution and aging treatment) on UFG formation with using RCMR processing was discussed. The changes in microstructure and crystallographic texture are studied and the mechanism of grain refinement was investigated.

2. Experimental procedure

Copper alloy with the addition of 0.6% wt. Cr (C18200) was used in this experiment. The alloy was prepared by melting and alloying in the open-air induction furnace, followed by casting into a mold with the diameter of 50 mm. The ingots were hot-rolled into rods with the diameter of 10 mm. The following heat treatment processes were applied to the samples in order to vary the initial structure prior to the RCMR deformation:

(1) solution treatment at 1000°C for 3 h followed by quenching into iced water. Only large precipitates were observed after the heat treatment. In this article referred to as: S.

* SILESIAN UNIVERSITY OF TECHNOLOGY, FACULTY OF MATERIALS ENGINEERING AND METALLURGY, 40-019 KATOWICE, KRASIŃSKIEGO STREET 8, POLAND
** WARSAW UNIVERSITY OF TECHNOLOGY, DEPARTMENT OF MATERIALS SCIENCE AND ENGINEERING, 02-507 WARSAW, WOŁOSKA STREET 141, POLAND
# Corresponding author: anna.urbanczyk-gucwa @polsl.pl

(2) solution and aging treatment at 500°C for 2 h. After applied heat treatment, the microstructure consisted of coherent second particles (Fig. 1). Referred to as: S1.
(3) solution and aging treatment at 700°C for 24 h. After applied heat treatment, the microstructure consisted of second particles with the dimension of about 270 nm. Referred to as: S2.

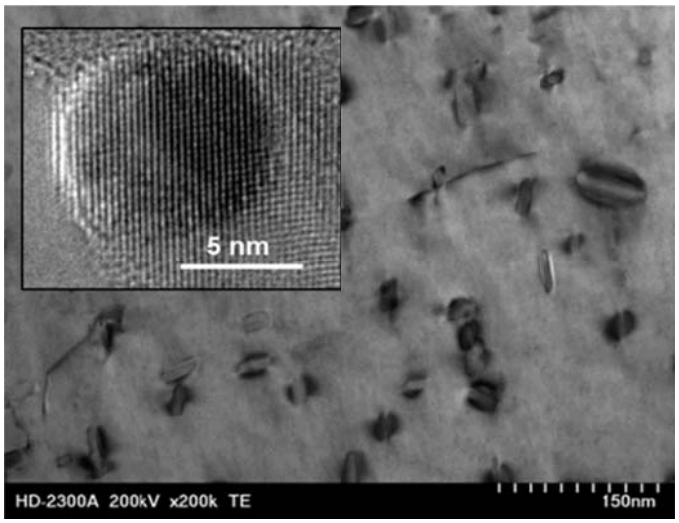

Fig. 1. Substructure of CuCr0.6 alloy after ageing in 500°C/2h

After the heat treatment, the samples were deformed by the RCMR method at room temperature. The total effective strain (ε_{fi}) in these experiments was 5. The details about RCMR method are given in [18]. The procedure for calculation of ε_{fi} is presented in [18]. All tests by using the RCMR method were conducted at room temperature. The samples in heat treated conditions and next deformed by RCMR are referred to as: S+RCMR; S1+RCMR and S2+RCMR.

Ultra-high resolution transmission electron microscope (TEM) TITAN 80-300 with field emission gun operated at 200 kV, and scanning transmission electron microscope (STEM) Hitachy HD-2300A with field emission gun operated at 200 kV were employed to investigate the detailed changes occurring in the microstructure. To examine the microstructure and texture evolution, the processed materials were taken from longitudinal section to the processing directions. The global texture investigations were performed using a Bruker D8 X-ray diffractometer applying filtered radiation Co Kα ($K\alpha_1$ = 0.1789 nm). The measurements were recorded within a 5×5° mesh and a beam intensity at 5 second intervals. Three incomplete X-ray pole figures ({111},{002},{022}) were used to evaluate complete Orientation Distribution Functions (ODFs) by spherical harmonics method and the Gauss model functions proposed by the Schultz reflection method [21]. The Labotex 2.1 software was used to calculate volume fraction of the main texture components [22]. It should be pointed out that a tolerance angle of 10° was used when the volume fractions were calculated.

Orientation distribution function (ODF) were calculated from the collected pole figures and subsequently qualitative (components) and quantitative (volume fraction) analysis of the preferential orientations were carried out. Orientations and misorientation of grains/subgrains have been determined by using Kikuchy diffraction method obtained by ultra-high resolution (S/TEM) scanning-transmission electron microscope TITAN 80-300. For orientation and misorientation calculation, KILIN program was used [23].

3. Results and discussion

Detailed research of the influence initial structure on microstructure formation and grain refinement were presented in [6,18]. The initial microstructure consists mainly of equiaxed grains with the average grain size of 72 mm.

Texture measurements were carried out to compare the crystal orientation of SPDed samples with different initial structure (with and without second particles).

In order to present the texture evolution and main texture components, ODFs were used for all investigated samples. A three-dimensional texture analysis with the use of ODF (derived from pole figures) were performed. Figure 2 represents the φ_2 = 0°, φ_2 = 45° and φ_2 = 60°, sections of the ODFs for the examined samples, where the most important preferential crystallographic orientations for f.c.c. materials may be found. Also, the main ideal texture position of components with theirs description were presented. Quantitative texture examinations of the material in the S state, indicates that the texture exhibits more randomly oriented crystallites (almost 70% of the volume fraction). In addition, a small fraction of <111> fiber can be distinguished as well as {0 0 1}<1 1 0> (rotated cube) and {1 1 1}<1 1 –2> components – their volume fraction amount to 8, 8, and 12 %, respectively. The components in Table 1 shows the selected typical and important texture in rolled and recrystallized metals. It should be noted, that the investigated materials after different heat treatment processes were deformed by the RCMR method. The {1 1 1}<1 1 –2> texture component, which was predominant in S+RCMR sample has undergone a significant broadening and weakening in second investigated material. As a result of the aging treatment and following deformation by the RCMR technique, weakening of the volume percentage of rotated cube component occurs, and additionally a {1 1 2}< 1 –1 0 > component is formed. The high level of background denotes formation of randomly oriented components in significant volume fraction. Weakness of the texture components may be explained by the formation of new, equiaxed grains with a small diameter.

The weakening of texture is the direct result of the grain refinement during SPD [14,15]. RCMR method can be beneficial for controlling the grain structure and texture of the deformed material. Our results demonstrated that this method of SPD is able to achieve the fine grained structure with a weak texture. Development of shear bands in severely deformed materials, may result in the texture weakening. As argued in [16] the fine recrystallized grains evolved in shear bands during can induced the weak basal texture. From literature it is known [14-16],

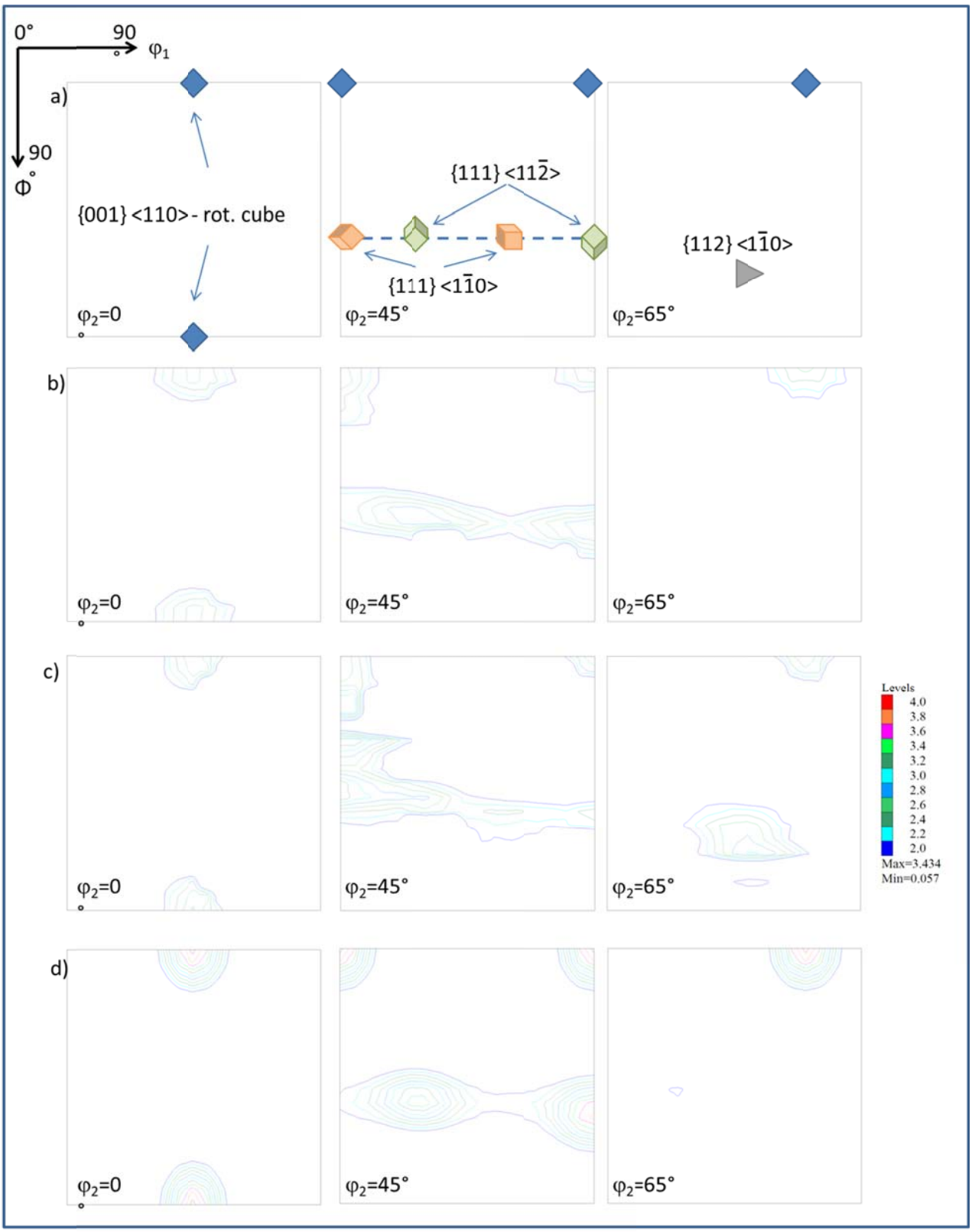

Fig. 2. ODFs at φ_2 = 0, 45 and 65° for some ideal orientations (a), S+RCMR sample (b), S1+RCMR sample (c) and S2+RCMR sample (d)

that samples subjected to the SPD by using selected techniques strongly suggested the evolution of dynamic recrystallized (DRX) grains, where during the dynamic recrystallization increase in boundary misorientations and conversion of LABs into HABs is observed. The cross-shear deformation can induce the formation of preferred nucleation sites for dynamic recrystallization during the DSR processing, leading to an increase in the fraction of DRX grains. It is well-known that DRX grains are oriented randomly and this situation leads to a basal texture weakening also [17]. Strain induced boundary migration was the

dominant mechanism of microstructure evolution in the alloy, which influenced the crystallographic texture development by weakening it [17].

After the final annealing, somewhat elongated grains with similar crystal orientations were arranged parallel to the rolling direction in the conventional process, whereas grains were smaller and more equiaxed with rather randomly arranged orientations in the ECAP process. Should be noted, that weakened basal texture itself is proposed to improve ductility.

In the sample after the longest time aging (S2+RCMR), the share of <111> fiber accounts to 16 % of volume fraction, whereas the fraction of the rotated cube component is a similar level as in the quenched sample (S+RCMR). Moreover, the counted volume fractions of the individual texture components and the ODF values give grounds to state that the texture of the S2+RCMR sample is formed more strongly than that of the S1+RCMR specimen. It worth to note, that combined heat treatment with RCMR caused a randomization of texture components in CuCr0.6 alloys.

The TEM characterization of RCMR deformed materials disclosed that the grain refining mainly occurred throughout the original grains subdivision by dislocation boundaries (Fig. 3).

As presented in Fig. 3, RCMR deformation revealed that the dislocation structure generally contained planar dense dislocation walls (DDWs) which are the products of geometrically necessary dislocations (GNDs) [24,25] (Fig. 3a,c). In the present study, one or two families of parallel DDWs were frequently observed (Fig. 3a). Some segments of these walls becoming high angle boundaries (Fig. 3a,c). Both roughly equiaxed subgrains (Fig. 3a,c,d) and elongated microbands (Fig. 3b) were observed within the deformation substructure using the TEM technique. Well-developed microbands with high angle boundaries became more dominant especially for samples in state 2 (Fig. 3b). In addition, high misorientation of nonequilibrium

TABLE 1

Volume fraction of the main texture components in the investigated materials

Texture component	Volume fraction of the main texture components in the investigated materials [%]		
	S+RCMR	S1+RCMR	S2+RCMR
<111> fiber	8	8	16
{0 0 1}<1 1 0> – rotated cube	8	3	8
{1 1 1}<1 1 –2>	12	1	7
{1 1 1}<1 –1 0>	3	2	1
{1 1 2}< 1 –1 0 >	0	14	0
Background	*69*	*72*	*69*

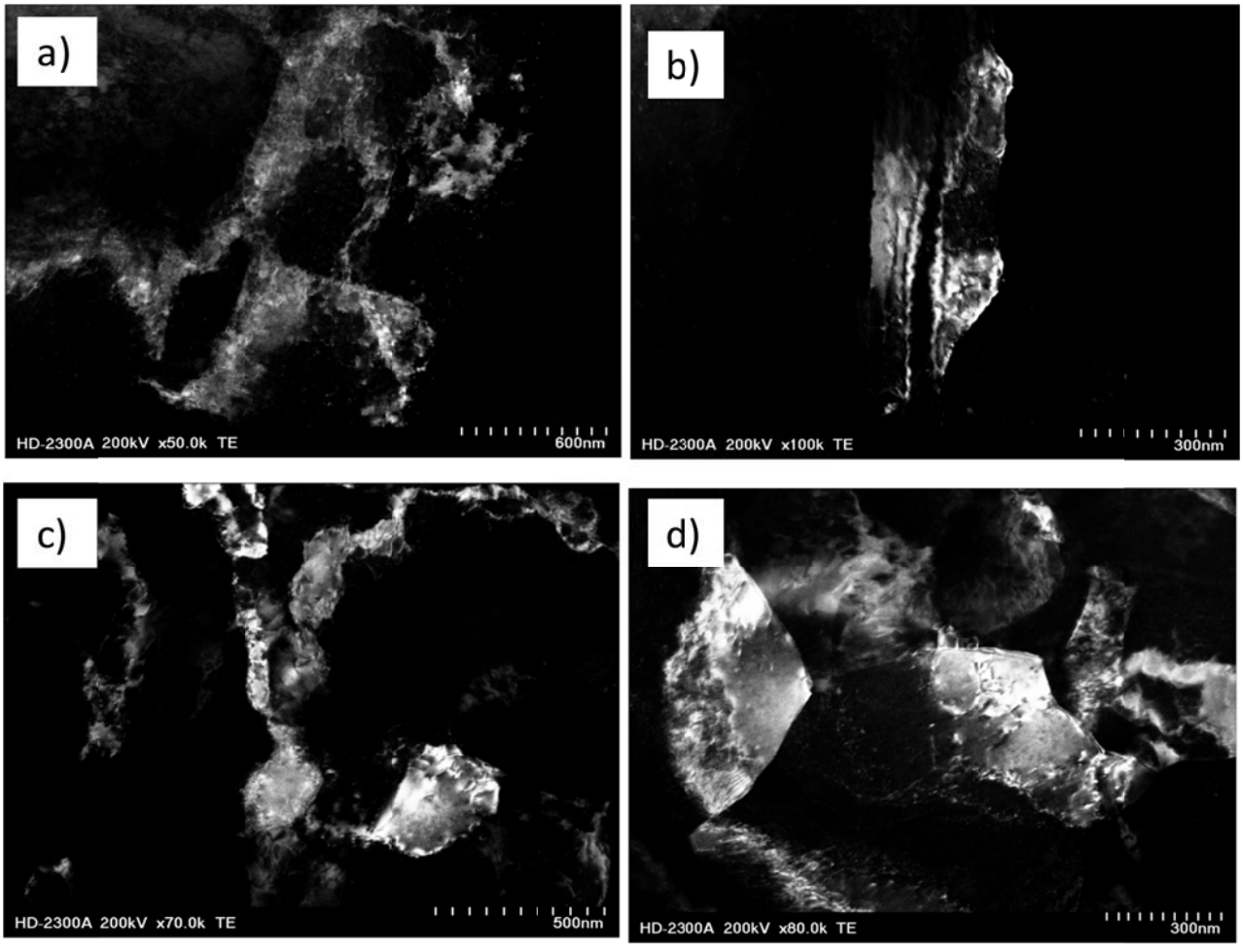

Fig. 3. Scanning transmission electron microscopy (STEM) dark field images of CuCr0.6 alloy in: a), S1+RCMR b) S2+RCMR

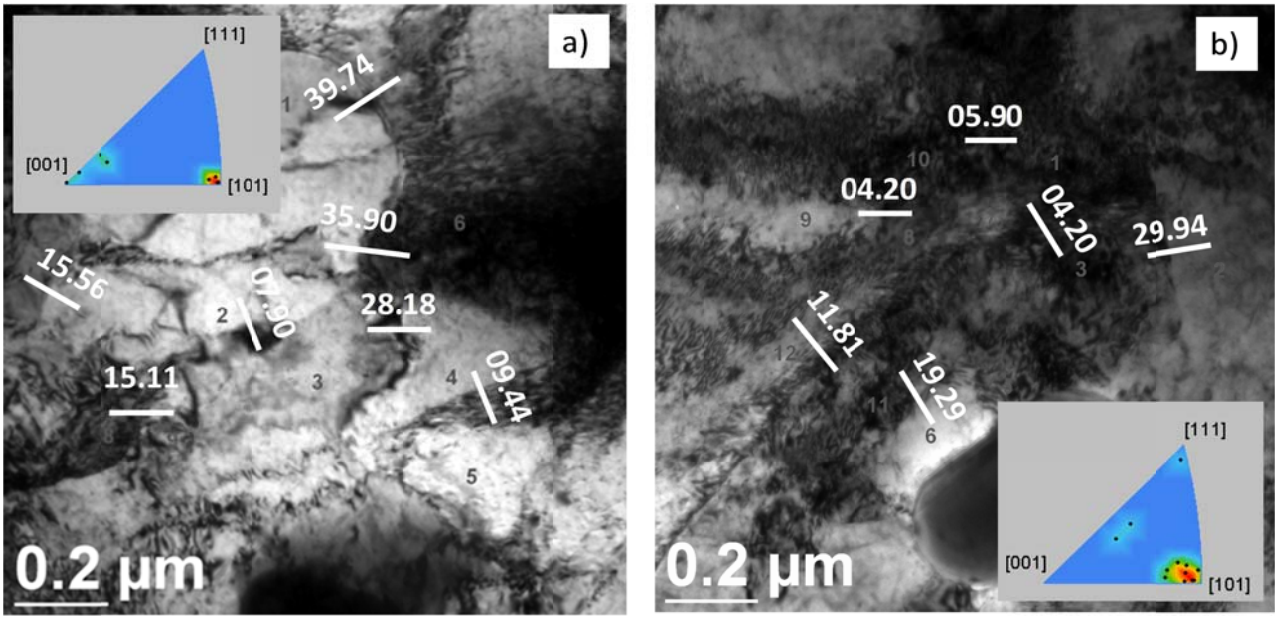

Fig. 4. Scanning transmission electron microscopy (STEM) dark field images of CuCr0.6 alloy in: a), b) S1+RCMR state

grain boundary were observed for sample S1+RCMR. Created grains are characterized by various crystallographic orientation (Fig. 4a). In areas of boundaries with high dislocation density confirmed increase of misorientation (Fig. 4b). Nonequlibrium grain boundary near precipitate is characterized by high angle boundaries.

For RCMR deformation incomplete transition of LAB to HAB have been observed, so in the results, grains with LAB and HAB are seen (Figs. 3,4).

Should be noted that process of grain refining proceeds by the generation of LABs which transform into HABs. In the initial state of deformation the dislocation boundaries are formed. With increase of deformation the number of the dislocation boundaries that cross mutually increase and the distances between the dislocation boundaries decrease. A significant role in the forming the ultrafine-grained structure has the recovery process [26]. Dislocations are rearranged, annihilated and are also absorbed to the grain boundaries. Such a rebuilding of a dislocation structure causes the increase of the misorientation of grain boundaries and transformation of these grain boundaries into nonequlibrium grain boundaries.

4. Conclusions

The evolution of crystallographic texture and deformation substructure was studied in CuCr0.6 alloy. Transmission electron microscopy (TEM) and diffractometer techniques were used in this investigations. In RCMR condition, continuous increase of misorientation between dislocation boundaries caused by the creation of non-equilibrium boundaries could be considered as the main mechanism to produce an UFG structure. The dislocations are generated and distributed in the initial stages of deformation. Subsequently, these distributed dislocations are replaced by subgrains bounded by LABs, and produce a finer cell/subgrain structures are observed. With the deformation, misorientation between cell/sugrain structures are increased continuously leading to creation of non-equilibrium grain boundaries and HABs formation. Cyclic character of deformation leads to an incomplete transition of LAB to HAB, so a high volume fraction of LAGB is seen. RCMR method is effective in weakening the deformed texture. The results obtained for samples S+RCMR, S1+RCMR and S2+RCMR did not show any significant difference in the evolution of the microstructure. RCMR processing of CuCr0.6 alloy demonstrates a nearly identical textural components.

Acknowledgements

The work was supported by the National Science Centre of Poland (project No. UMO-2013/09/B/ST8/01695).

REFERENCES

[1] A. Mishra, V. Richard, F. Grégori, R.J. Asaro, M.A. Meyers, Mater. Sci. Eng. A **410-411**, 290-298 (2005). DOI: 10.1016/J.MSEA.2005.08.201

[2] R.K. Islamgaliev, V.D. Sitdikov, K.M. Nesterov, D.L. Pankratov, Rev. Adv. Mater. Sci. **39**, 61-68 (2014).

[3] J. Bogucka, Arch. Metall. Mater. **59**, 127-131 (2014). DOI: 10.2478/amm-2014-0020

[4] K. Edalati, K. Imamura, T. Kiss, Z. Horita, Mater. Trans. **53**, 123-127 (2012). DOI: 10.2320/matertrans.MD201109

[5] R.Z.V. R.K. Islamgaliev, K.M. Nesterov, J. Bourgon, Y. Champion, J. Appl. Physic. **115**, 194301-194304 (2014).

[6] K. Rodak, A. Brzezińska, R. Molak, Mater. Sci. Eng. A (2018). DOI: 10.1016/j.msea.2018.03.077

[7] W. Głuchowski, J. Domagała-Dubiel, J. Sobota, J. Stobrawa, Z. Rdzawski, Arch. Mater. Sci. Eng. **60**, 53–63 (2013).

[8] B. Tolaminejad, A.K. Taheri, M. Shahmiri, H. Arabi, Int. J. Mod. Phys. Conf. Ser. **05**, 325-334 (2012). DOI: 10.1142/S201019451200219X

[9] P.Z. Rodak K., Molak R.M., Phys. Status Solidi C-Curent Top. Solid State Phys. **7**, 1351-1354 (2010).

[10] A.L. Etter, T. Baudin, C. Rey, R. Penelle, Mater. Charact. **56**, 19–25 (2006). DOI: 10.1016/j.matchar.2005.09.003

[11] V.M. Segal, Mater. Sci. Eng. A **406**, 205–216 (2005). DOI: 10.1016/J.MSEA.2005.06.035

[12] L.S. Tóth, B. Beausir, C.F. Gu, Y. Estrin, N. Scheerbaum, C.H.J. Davies, Acta Mater. **58**, 6706-6716 (2010). DOI: 10.1016/J.ACTAMAT.2010.08.036

[13] A.D. Kammers, T.G. Langdon, **29**, 1664-1674 (2014). DOI: 10.1557/jmr.2014.207

[14] H. Lanjewar, L. Kestens, P. Verleysen, EPJ Web Conf. **183**, 03008 (2018). DOI: 10.1051/epjconf/201818303008

[15] J. Yan, J. Ma, J. Wang, Y. Shen, Metall. Mater. Trans. A **49**, 5333–5338 (2018). DOI: 10.1007/s11661-018-4874-y

[16] K. Hamad, Y.G. Ko, Sci. Rep. **6**, 29954 (2016). DOI: 10.1038/srep29954

[17] N. Nadammal, S.V. Kailas, J. Szpunar, S. Suwas, Mater. Charact. **140**, 134-146 (2018). DOI: 10.1016/j.matchar.2018.03.044

[18] K. Rodak, A. Urbańczyk-Gucwa, M.B. Jabłońska, Arch. Civ. Mech. Eng. **18**, 500-507 (2018). DOI: 10.1016/j.acme.2017.07.001

[19] A. Urbańczyk-Gucwa, K. Rodak, A. Płachta, J. Sobota, Z. Rdzawski, Characteristic structure of Cu-0.8Cr alloy using SPD deformation by rolling with cyclic movement of rolls method, 2016. DOI: 10.4028/www.scientific.net/KEM.682.3

[20] K. Rodak, A. Urbańczyk-Gucwa, K. Radwański, A. Phys. Pol. A. **130**, (2016). DOI: 10.12693/APhysPolA.130.1151

[21] L.G. Schulz, J. Appl. Phys. **20**, 1030-1033 (1949). DOI: 10.1063/1.1698268

[22] http://www.labosoft.com.pl, (b.d.).

[23] B.A. Richter, K. Chruściel, J. Długopolski, (b.d.).

[24] D. Hughes, N. Hansen, Acta Mater. **48**, 2985-3004 (2000). DOI: 10.1016/S1359-6454(00)00082-3

[25] X. Huang, Scr. Mater. **38**, 1697-1703 (1998). DOI: 10.1016/S1359-6462(98)00051-7

[26] K. Rodak, J. Pawlicki, Mater. Charact. (2014). DOI: 10.1016/j.matchar.2014.05.002